



Contents lists available at ScienceDirect

Bioorganic & Medicinal Chemistry

journal homepage: www.elsevier.com/locate/bmc

Synthesis and profiling of benzylmorpholine 1,2,4,5-tetraoxane analogue N205: Towards tetraoxane scaffolds with potential for single dose cure of malaria

Paul M. O' Neill^{a,*}, Paul A. Stocks^a, Sunil Sabbani^a, Natalie L. Roberts^a, Richard K. Amewu^{a,f}, Emma R. Shore^a, Ghaith Aljayyousi^b, Iñigo Angulo-Barturén^c, María Belén^c, Jiménez-Díaz^c, Santiago Ferrer Bazaga^c, María Santos Martínez^c, Brice Campo^d, Raman Sharma^b, Susan A. Charman^e, Eileen Ryan^e, Gong Chen^e, David M. Shackelford^e, Jill Davies^b, Gemma L. Nixon^a, Giancarlo A. Biagini^b, Stephen A. Ward^b

^a Department of Chemistry, University of Liverpool, Liverpool L69 7ZD, United Kingdom

^b Research Centre for Drugs and Diagnostics, Liverpool School of Tropical Medicine, Pembroke Place, Liverpool L3 5QA, United Kingdom

^c Tres Cantos Medicines Development Campus, DDW, GlaxoSmithKline, Severo Ochoa 2, 28760 Tres Cantos, Spain

^d Medicines for Malaria Venture, ICC, Route de Pré-Bois 20, P.O. Box 1826, 1215 Geneva, Switzerland

^e Centre for Drug Candidate Optimisation, Monash Institute of Pharmaceutical Sciences, Monash University, 381 Royal Parade, Parkville, VIC 3052, Australia

ARTICLE INFO

Article history:

Received 30 January 2018

Revised 3 May 2018

Accepted 4 May 2018

Available online xxx

ABSTRACT

A series of aryl carboxamide and benzylamino dispiro 1,2,4,5-tetraoxane analogues have been designed and synthesized in a short synthetic sequence from readily available starting materials. From this series of endoperoxides, molecules with *in vitro* IC₅₀s versus *Plasmodium falciparum* (3D7) as low as 0.84 nM were identified. Based on an assessment of blood stability and *in vitro* microsomal stability, N205 (**10a**) was selected for rodent pharmacokinetic and *in vivo* antimalarial efficacy studies in the mouse *Plasmodium berghei* and *Plasmodium falciparum* Pf3D70087/N9 severe combined immunodeficiency (SCID) mouse models. The results indicate that the 4-benzylamino derivatives have excellent profiles with a representative of this series, N205, an excellent starting point for further lead optimization studies.

© 2018 Published by Elsevier Ltd.

1. Introduction

The emergence of malaria parasite resistance to most available drugs,¹ including the semi-synthetic artemisinin derivatives artemether and artesunate,^{2–4} has led to efforts to create new synthetic peroxides as potential antimalarial agents. Leading examples of synthetic endoperoxides include OZ277 (arterolane) (**1**),⁵ a molecule deployed in combination with piperazine (known as Synriam),⁶ and OZ439 (**2**) a second generation deriva-

tive with improved pharmacokinetics and enhanced *in vivo* antimalarial activity.^{7–9} 1,2,4,5-Tetraoxanes are another class of peroxide with excellent antimalarial profiles against both chloroquine-resistant and chloroquine-sensitive strains of *Plasmodium falciparum* and oral activity in murine models of the disease.^{10–15} Previously in our group, RKA182 (**3**) (Fig. 1) was selected as a candidate for full preclinical development from a series of synthetic tetraoxane derivatives; this compound shows superior *in vitro* and *in vivo* activity compared to artemether and artesunate, has good oral bioavailability in rodent models and is more stable than arterolane in malaria infected human red blood cells.^{16,17} Although the PK profile for RKA182 is compatible with that of a 3-day dosing regimen, there is now a drive for the development of endoperoxides with PK/PD properties predicted to allow single dose cure in humans. Three distinct tetraoxane templates were simultaneously investigated; a representative described here, alongside the series which led to the discovery of E209 (**4**)^{17,18}, both of which have PK/PD characteristics that are compatible with a single-dose cure (See Scheme 1).

Abbreviations: AUC, area under the curve; BA, bioavailability; CL_{plasma}, plasma clearance; CL_{int}, intrinsic clearance; CYP, cytochrome P450; DCM, dichloromethane; DMF, dimethyl formamide; ED, effective dose; FaSSIF, fasted state simulated intestinal fluid; FeSSIF, fed state simulated intestinal fluid; IC, inhibitory concentration; IV, intravenous; LAH, lithium aluminium hydride; PD, pharmacodynamic; PK, pharmacokinetic; PO, oral; SCID, severe combined immunodeficiency; THF, tetrahydrofuran; Vdss, volume of distribution at steady state.

* Corresponding author.

E-mail address: p.m.oneill01@liv.ac.uk (P.M. O' Neill).

^f Present address: Department of Chemistry, University of Ghana, P. O. Box LG56, Legon, Ghana, Accra.

<https://doi.org/10.1016/j.bmc.2018.05.006>

0968-0896/© 2018 Published by Elsevier Ltd.

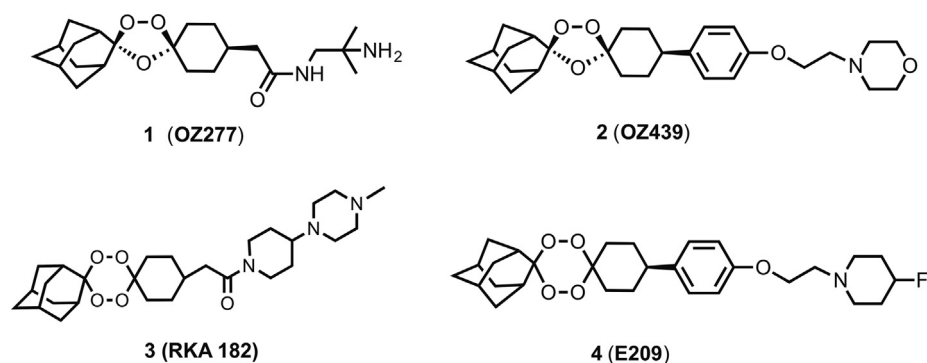
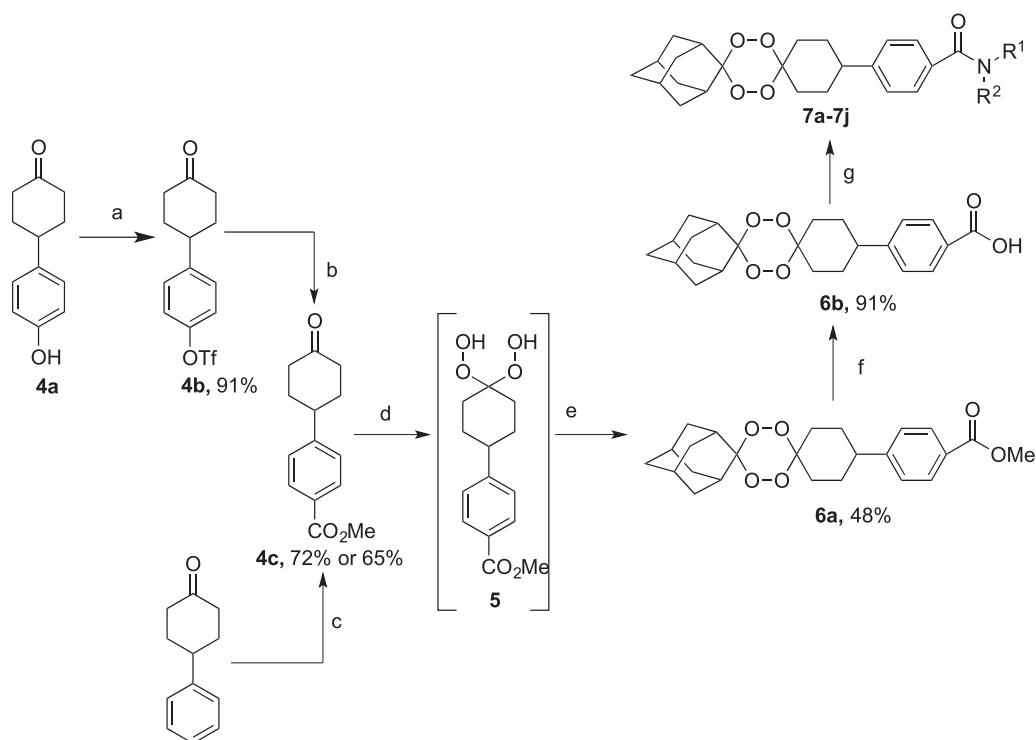
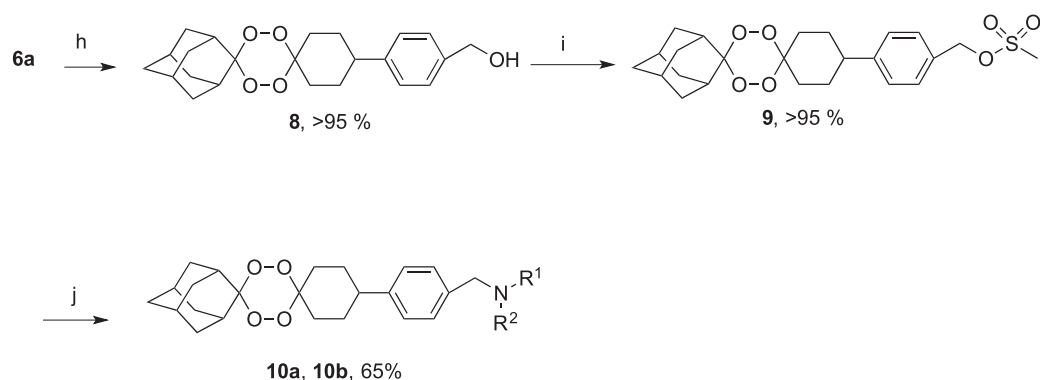


Fig. 1. Structures of synthetic peroxides OZ277, OZ439, RKA182 and E209.

A) Amide Analogues



B) Amine Analogues



Scheme 1. (a) TiF_2O , NEt_3 , -25°C –rt, 12 h, (b) $\text{Pd}(\text{OAc})_2$, CO, atm, DIPEA, dppp, DMF/MeOH, 70°C , 5 hr, rt, o/n, (c) oxalyl chloride, AlCl_3 , DCM, 0°C –rt o/n, 0°C , MeOH, pyridine, rt, 3 h, (d) Formic acid/HCl, 50% H_2O_2 , acetonitrile, 0°C , 30–60 min (e) 2-adamantanone, Re_2O_7 , DCM, rt, 1 h (f) MeOH, KOH, 70°C (g) NEt_3 , 0°C , CH_3COCl , 1 h, NHR^1R^2 , 0°C , 30 min then rt, 1.5 h (h) THF, LAH, 0°C , 30 min (i) NEt_3 , THF, 0°C , methanesulfonyl chloride, 1.5 h (j) NEt_3 , DCM, 0°C , 10 min, then amine, rt 3.5 h.

2. Results and discussion

Herein we describe the design and synthesis of a new series of tetraoxanes (Templates 1 and 2, Fig. 2) and present data on their *in vitro* and *in vivo* antimalarial activity profiles. The new series were designed to increase the lipophilicity (CLogP/LogD) compared with RKA182 (by inclusion of an aromatic ring in the side-chain) and enhance blood stability (rodent and human) in addition to enhancing PK/PD properties in appropriate animal models. For the benzyl series, we focused on the use of morpholine and fluoro-piperidine to enable direct comparisons with OZ439 and E209.

2.1. Chemistry

Two routes were explored for the synthesis of key ester **4c**. Initially, we examined the conversion of commercially available 4-(4-hydroxyphenyl)cyclohexanone **4a** into the corresponding triflate **4b**. This was then subjected to a palladium mediated carbonylation reaction in the presence of methanol to provide methyl ester **4c**. This key intermediate could be converted into the tetraoxane ester **6** according to the procedure developed by Dussault et al.¹⁹ An alternative approach to **4c** involves the use of a modified Friedel-Crafts procedure on 4-phenyl cyclohexanone; this latter route has advantages in terms of scale up of chemistry for production of multi-gram quantities. For the synthesis of template 1 analogues the ester **6** was first hydrolysed to the carboxylic acid **6b** and converted to target amides via a mixed anhydride intermediate. For template 2 analogues, the ester **6** was reduced with LAH to the alcohol **8** and treated with methane sulfonyl chloride to form the mesylate **9** which was then allowed to react with morpholine (or 4-fluoro cyclohexanone for N214, **10b**).

2.2. Biological assessment

All compounds synthesized were tested *in vitro* against the 3D7 strain of *Plasmodium falciparum*.²⁰ With the exception of the amino cyclobutane **7d** and thiomorpholine analogue **7e**, all of the tetraoxane analogues displayed potent single digit nanomolar activity with several compounds more potent than OZ439 positive control. No correlation was seen with calculated physicochemical parameters such as CLogP, LogD or calculated solubility (Table 1) consistent with previous reports for trioxolane derivatives.^{5,8} Due to the importance of blood stability for enhancing overall drug exposure in this class, compounds depicted in Table 1 were screened for stability in human and rat blood and it was shown that the amide series was unstable particularly in rat blood (half-life < 4 h, data not shown). Amides **7h**, and **7i** (all of which have higher ClogP values than RKA182) were selected for *in vivo* analysis along with the benzylamino analogues **10a** and **10b** (the latter compounds demonstrated comparatively better rodent and human blood stability).

Data presented in Table 2 summarise the results in terms of cure and mean survival time following a single 30 mg/kg oral dose treatment of *Plasmodium berghei* (*P. berghei*) infected mice. The performance of the amides, although superior to artesunate and equivalent to RKA182 and OZ277, was comparatively poor relative to OZ439. In contrast, the benzylamino analogues performed better than the amides with a 26 day mean survival for N205 (**10a**) and 13 day average survival for fluoropiperidine analogue **10b**. For the benzyl morpholine analogue N205, 2/3 mice were cured; use of the mesylate salt of N205 in a standard suspension vehicle (SSV) was next examined to see if a better performance could be obtained with the salt form. A similar result was obtained with a 66% single dose cure rate and average survival of 25 days. Snapshot PK data for this latter study revealed significant levels of N205 in

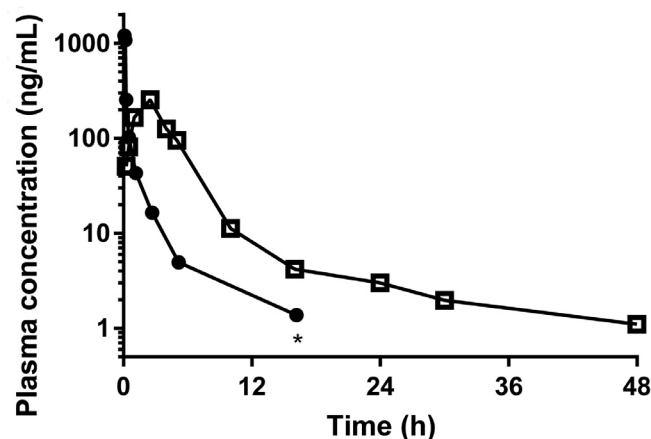


Fig. 2. Plasma concentrations in male Sprague Dawley rats following IV and PO administration of 1.6 and 8.1 mg/kg, respectively. Data represent the mean of $n = 2$ rats except for the point marked with * where only one measurement was available.

the plasma at the 24 h timepoint (>100 ng/ml). These results are superior data recorded for the tetraoxane version of OZ439 tested previously in the same animal model where the mean survival was 15 days with no cures²¹. Based on these results, N205 was selected for more extensive profiling to determine if comparative studies should be performed in the humanized mouse model of malaria. OZ439 was used as the benchmark compound throughout these studies.

Table 3 shows data for the measured solubility of the mesylate salt of N205. Compound **10a** is more soluble in water than OZ439 mesylate but is less soluble in 0.01 and 0.1 M HCl, FaSSIF and FeSSIF media. Overall, the profile points towards lower overall solubility than OZ439 (it should be noted that the final salt form and levels of crystallinity will influence solubility data in these assays).

N205 (**10a**) exhibited degradation in human, rat and mouse liver microsomes with rates generally being fastest in rat and slowest in mouse (Table 4). The rates of degradation were similar in human and rat liver microsomes at substrate concentrations of 1 and 5 μ M, however the rate of degradation in mouse liver microsomes appeared to be somewhat lower at the higher substrate concentration suggesting a possible concentration dependency.

Metabolite identification (see Supplementary Material) for N205 revealed that the major route of metabolism for N205 is hydroxylation of the adamantane ring accounting for almost 50% of the turnover observed in human liver microsomes (based on peak area only). Minor metabolites observed included products stemming from tetraoxane ring cleavage (M-182) and morpholine ring cleavage (M-26). Thus the metabolic weak spot in these structures is the lipophilic adamantane ring system and improvement in the DMPK profile may be possible through chemical substitution within the adamantylidene portion of the molecule.

As noted previously, an important feature of OZ439 is its enhanced blood stability⁷ thought to be due at least in part to reduced degradation in the presence of Fe(II). Table 5 shows data on the stability in human and rat blood, predicted plasma clearance and rat pharmacokinetic data for N205 and OZ439. N205 has similar human blood stability compared to OZ439 but is less stable in rat blood with a measured half-life of approximately 8 h. The high plasma protein binding for both N205 and OZ439 in human plasma may have some impact on the observed blood stability and further studies are in progress to explore this. Predicted human clearance values for OZ439 and N205 are similar with higher clearance predicted in rats for the tetraoxane analogue.²² In head to head comparisons of tetraoxanes with 1,2,4-trioxolanes in our laboratory, it is generally observed that rodent microsomal

Table 1*In vitro* 3D7 IC₅₀, CLogD, calculated solubility, CLog P.

Compound	Structure	IC ₅₀ 3D7 (nM)	CLogD ^a 7.4	Calculated ^a Solubility (mg/mL)	ClogP ^a
7a		7.1 ± 0.4	3.96	0.02	3.22 ± 0.81
7b		5.3 ± 0.6	1.31	0.029	4.66 ± 0.80
7c		0.84 ± 0.03	1.36	0.083	3.85 ± 0.80
7d		33.0 ± 1.0	1.11	0.013	2.59 ± 0.80
7e		15.0 ± 1.0	4.58	0.01	4.10 ± 0.90
7f		6.4 ± 0.6	3.93	0.10	3.68 ± 0.84
7g		0.82 ± 0.11	1.70	0.034	3.61 ± 0.84
7h		3.0 ± 0.4	2.76	0.13	3.18 ± 0.86
7i		4.2 ± 0.45	1.11	0.027	3.37 ± 0.79
7j		1.10 ± 0.1	1.07	0.69	3.39 ± 0.90
10a (N205)		1.3 ± 0.1	4.42	0.076	4.50 ± 0.82
10b (N214)		1.8 ± 0.7	5.02	0.025	5.36 ± 0.86
OZ439		8.0 ± 0.3	4.83	0.55	4.63 ± 0.70

^aLog D, log P and Solubility values were calculated using the Virtual Computational Chemistry Laboratory (VCCLAB); <http://www.vcclab.org>.**Table 2**Percentage activity and mean mouse survival time following 30 mg/kg single oral dose in the *P. berghei* model.

Compound Number	% Activity	Mean survival time (days) following 30 mg/kg oral dose
7h	99.0	10.0 (9, 10, 11)
7i	99.0	8.0 (8, 8, 8)
10a (N205)	99.42	26.3 (16, 30, 30)
10a (N205 mesylate)	99.30	25.0 (15, 30, 30)
10b (N214 mesylate)	99.98	13 (12, 13, 14)
OZ277	99.98	10.2 (8, 10, 8, 10, 15)
RKA182	99.98	11.4 (14, 15, 7, 7, 14)
OZ439	99.40	30 (30, 30, 30)
Artesunate	99.09	6.8 (6, 7, 7, 7, 7)
Untreated Control	–	4.0 (4, 4, 4)

clearance is faster for the adamantylidene tetraoxane scaffold. The higher predicted rat hepatic clearance and lower rat blood stability translates into a comparatively worse performance for N205 in terms of rat pharmacokinetics (Table 5 and Fig. 2). N205 exhibited higher clearance and lower oral bioavailability of 52% compared

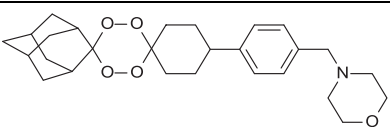
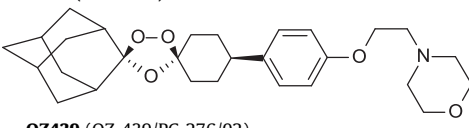
Table 3Overall solubility results for N205 (**10a**) mesylate at 37 °C after 4 h. All solubility values refer to the free base equivalent.

Medium	Solubility (µg/mL) after 4 h at 37 °C	
	OZ439 mesylate	N205 mesylate
Water	6800	>9000
pH 2.0 buffer	>8000	>9000
0.1 N HCl pH 1.0	34	17
0.01 N HCl pH 2.0	240	172
pH 7.4 PBS	Not meas.	<0.1
FaSSIF pH 6.5	120	18
FeSSIF pH 5.0	>1500	760

Both plasma and microsomal protein binding of N205 and OZ439 were found to be very high (>99.9% bound for both compounds in each matrix).

with approximately 100% for OZ439. Both IV and PO half-lives of OZ439 were superior to N205, although the 17 h oral half-life of N205 demonstrates a large improvement over all other endoperoxides examined in this class (e.g. PO half-life of RKA182 at same dose was 3.5 h).¹⁶

Table 4*In vitro* Metabolism in Liver Microsomes.

Compound Details	Species	Substrate Concentration (μM)	Degradation half-life (min)	<i>In vitro</i> CL _{int} (μL/min/mg protein)	Microsome-Predicted E _H
 N205 (CDCO_01)	Human	1	34 (33, 35)	51 (53, 50)	0.67 (0.68, 0.66)
		5	43 (44, 41)	41 (39, 42)	0.62 (0.61, 0.63)
	Rat	1	15 (13, 16)	118 (130, 105)	0.75 (0.77, 0.73)
		5	20 (17, 23)	89 (101, 76)	0.69 (0.72, 0.66)
	Mouse	1	48 (42, 54)	37 (41, 32)	0.44 (0.47, 0.41)
		5	87 (93, 82)	20 (19, 21)	0.30 (0.29, 0.31)
 OZ439 (OZ-439/PC-276/02)	Human	1	25 (26, 23)	71 (66, 75)	0.74 (0.72, 0.75)
		5	66 (73, 59)	27 (24, 29)	0.51 (0.49, 0.54)
	Rat	1	95 (86, 103)	18 (20, 17)	0.32 (0.34, 0.30)
		5	141 (75, 207)	16 (23, 8)	0.27 (0.37, 0.18)
	Mouse	1 ^a	126	14	0.23
		5	197	9	0.16

Data represent the mean values of two technical replicates (individual values in parenthesis), except for OZ439 in mouse liver microsomes where only one value is available.

^aData reported previously.²¹**Table 5**Human/rat blood stability, predicted plasma clearance and rat pharmacokinetic parameters of N205 versus OZ439. PK parameters for OZ439 are from⁷.

Property	N205 Mesylate	OZ439 mesylate
<i>In vitro</i> blood stability (37 °C, 4 h)		
T _{1/2} (h) in rat blood	~8	>15
T _{1/2} (h) in human blood	~10% loss	No degradation detected
Pred CL _{plasma} (mL/min/mg)*		
Human	14	15
Rat	50	21
Mouse	53	28
Rat PK		
CL _{plasma} (mL/min/kg)	77	40
Vdss (L/kg)	11	18
Estimated IV T _{1/2} (h)BA (%)	6.352	32
		~100

Additional profiling in human liver microsomes to determine CYP450 inhibition (Table 6) revealed no concerns (IC₅₀ > 20 μM for each isoform).

In order to provide an assessment of the therapeutic efficacy of N205 against *P. falciparum* Pf3D70087/N9, potency was assessed by administering a single oral dose (2.5, 5, 15, 30, 50 and 100 mg·kg⁻¹) at day 3 after infection and measuring the effect on blood parasitemia by flow cytometry (Fig. 3A–C and Table 7).^{23,24} The parameters of efficacy estimated in the study were a) the dose of N205 that reduces parasitemia at day 7 after infection by 90% with respect to vehicle-treated mice (parameter denoted as ED₉₀) and b) the estimated average daily exposure in whole blood necessary to reduce *P. falciparum* parasitemia in peripheral blood at day 7 after infection by 90% with respect to vehicle-treated mice (parameter used to measure the potency of the compound and denoted as AUC_{ED90}). In the experimental conditions used in the assay N205 is efficacious against *P. falciparum*, with ED₉₀ = 8.6 mg·kg⁻¹ and

Table 6IC₅₀ values against five drug-metabolising CYP isoforms using a substrate specific approach in human liver microsomes.

CYP isoform	IC ₅₀ (μM)	
	N205	Reference Inhibitor
CYP1A2	>20	3.6 (Furafylline)
CYP2C9	>20	0.72 (Sulfaphenazole)
CYP2C19	>20	0.48 (Ticlopidine)
CYP2D6	>20	0.025 (Quinidine)
CYP3A4 (Midazolam 1'-hydroxylation)	>20	0.022 (Ketoconazole)
CYP3A4 (Testosterone 6β-hydroxylation)	>20	0.013 (Ketoconazole)

AUC_{ED90} < 0.75 μg·h·ml⁻¹ following single oral dose administration. In contrast to studies in *P. berghei*, the dose levels administered were not able to cure mice even at the top dose of 100 mg/kg. The *in vivo* data confirms that N205 has outstanding antimalarial activity within the same region as OZ439 and E209.^{7,18} In this model, an ED₉₀ of 10 mg/kg was obtained for artesunate after four daily doses indicating that a single dose of N205 has similar oral potency to multiple doses of artesunate.

3. Experimental methods

3.1. Biological assessment

Please see [Supplementary Information](#) for solubility, plasma protein binding and blood stability experimental methods.

3.1.1. *In vitro* sensitivity assays

Drug susceptibilities were assessed at the Liverpool School of Tropical Medicine by the measurement of fluorescence after the addition of SYBR Green I as previously described by Smilkstein et al.²⁰ Drug IC₅₀s were calculated from the log of the dose/response relationship as fitted with Graft software (Erithacus Software, Kent, United Kingdom). Results are given as the mean of at least three separate experiments.

For the fluorescence assay, after 48 h of growth, 100 μl of SYBR Green I in lysis buffer (0.2 μl of SYBR Green I/ml of lysis buffer) was added to each well, and the contents were mixed until no visible erythrocyte sediment remained. After 1 h of incubation in the dark at room temperature, fluorescence was measured with a Varioskan fluorescence multiwell plate reader from Thermo Electron Corporation with excitation and emission wavelengths of 485 and 530 nm, respectively.

3.1.2. *In vitro* physicochemical and ADME studies and *in vivo* animal experiments

3.1.2.1. *In vitro* ADME and *in vivo* PK. The *in vitro* ADME studies and *in vivo* PK studies were conducted at the Centre for Drug Candidate Optimisation, Monash University (Australia). Methods for solubility, metabolite identification, plasma and microsomal protein binding, and plasma analysis are described in the [Supplementary Information](#). Microsomal stability and CYP inhibition were conducted as described previously²⁵ using liver microsomes from Sekisui XenoTech (Kansas City, KS). Rat PK and rat blood stability studies were performed as described previously⁷ in accordance with the Australian Code of Practice for the Care and Use of Animals for Scientific Purposes, and the study protocols were approved by the Monash Institute of Pharmaceutical Sciences Ani-

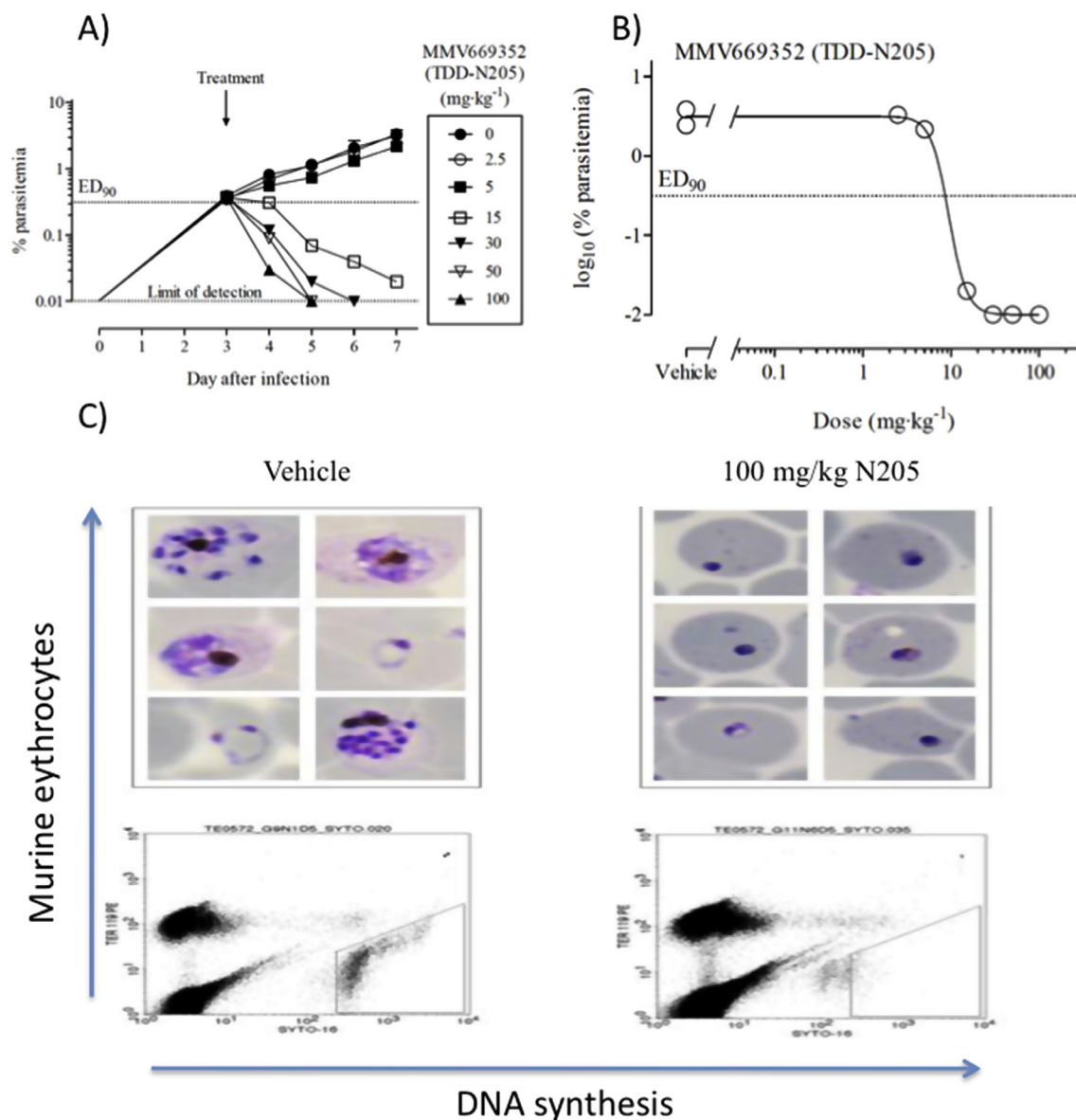


Fig. 3. (A) Parasitemia in peripheral blood of mice infected with *P. falciparum* Pf3D70087/N9. Data shown correspond to individual parasitemia values for mice treated with N205 or vehicle ($n = 2$). (B) Dose-response relationship for N205; data are presented as \log_{10} [percentage of parasitemia at day 7 after infection] of individual mice versus the dose in $\text{mg}\cdot\text{kg}^{-1}$. Parasitemias lower than the limit of detection of flow cytometry (0.01%) are computed and plotted as 0.01% for the dose-response curve fitting. (C) Upper panels show peripheral blood smears stained with Giemsa and lower panels show flow cytometry dot plots from samples of peripheral blood stained with TER-119-Phycoerythrin and SYTO-16. Dots inside the polygonal region represent *P. falciparum*-infected human erythrocytes.

Table 7
PK Parameters for N205 in the humanized *Pf* SCID mouse model at five different doses.

Blood PK Parameters in humanized mouse					
Dose (mg/kg)	5	15	30	50	100
C_{max} ($\mu\text{g}/\text{mL}$)	0.1090	0.1480	0.1480	0.6070	0.2500
$C_{\text{max}}/\text{Dose}$ ($\mu\text{g}/\text{mL}$ per mg/kg)	0.0218	0.0099	0.0049	0.0121	0.0025
t_{max} (h)	1	1	1	2	0.5
$\text{AUC}_{(0-t)}$ ($\mu\text{g}\cdot\text{h}/\text{mL}$)	1.2801 ^a	0.7489 ^b	0.9399 ^b	2.9973 ^b	2.3211 ^c
$\text{DNAUC}_{(0-t)}$ ($\mu\text{g}\cdot\text{h}/\text{mL}$ per mg/kg)	0.2560	0.0499	0.0313	0.0599	0.0232
Efficacy Parameters in humanized mouse					
ED_{90} $\text{mg}\cdot\text{kg}^{-1}$					8.6/6.2*
AUC_{ED90} $\mu\text{g}\cdot\text{h}\cdot\text{mL}^{-1}$					<0.75/0.68*
AUC_{PCC} $\mu\text{g}\cdot\text{h}\cdot\text{mL}^{-1}$					-/-*

^a $t = 4$ h; ^b $t = 8$ h; ^c $t = 23$ h; ^d DNAUC, dose normalized AUC_{0-t} *data for OZ439.

mal Ethics Committee. The intravenous formulation for N205 was prepared in 5% w/v glucose solution, whilst the oral formulation was prepared as a solution in aqueous vehicle containing 0.5% w/v hydroxypropylmethyl cellulose, 0.5% v/v benzyl alcohol and 0.4% v/v Tween 80.

3.1.2.2. In vivo antimalarial screening (*Plasmodium berghei*). In vivo efficacy studies in *P. berghei*-infected mice were conducted at the Swiss Tropical and Public Health Institute (Basel, Switzerland), adhering to local and national regulations of laboratory animal welfare in Switzerland (permission No. 1731). The tetraoxanes and OZ439 were dissolved or suspended in a vehicle consisting of 0.5% w/v hydroxypropylmethyl cellulose, 0.5% v/v benzyl alcohol, 0.4% v/v Tween 80, and 0.9% w/v sodium chloride in water, and administered orally on day 1 post infection. Antimalarial activity was measured as a percent reduction in parasitemia on day 3

post infection. Animals were considered cured if there were no detectable parasites on day 30 post infection. The onset of action was determined after a single oral dose of compounds to mice ($n = 3$) on day 3 post infection, resulting in a high initial parasitemia to allow the onset of action to be assessed. The reduction in parasitemia was initially monitored at 12 h post treatment, and the time of recrudescence was assessed by daily blood smears for 14 d followed by intermittent assessment up to 30 days. All groups, including an untreated control group, were infected simultaneously with *P. berghei*. Parasitemia was determined on day 3 post infection, and compared with values in control animals.

3.1.2.3. In vivo efficacy (Pf SCID mice). Humanised mouse efficacy and pharmacokinetic studies in Pf SCID mice were conducted at GSK Tres Cantos, Madrid. Studies of murine *P. falciparum* infection were ethically reviewed and carried out in accordance with European Directive 2010/63/EU and the GSK Policy on the Care, Welfare and Treatment of Laboratory Animals. *In vivo* efficacy against *P. falciparum* was conducted²³ in age-matched female immunodeficient NOD.Cg-Prkdcscid Il2rgtm1Wjl/SzJ mice (8–10 weeks of age; 22–24 gm) supplied by Charles River, UK, under license of The Jackson Laboratory, Bar Harbor. Mice were engrafted with human erythrocytes (Red Cross Transfusion Blood Bank in Madrid, Spain) by daily intraperitoneal injection with 1 mL of a 50% hematocrit erythrocyte suspension (RPMI 1640 (Invitrogen), 25 mM HEPES (Sigma), 25% decompartmented AB+ human serum (Sigma) and 3.1 mM hypoxanthine (Sigma)). Mice with ~40% circulating human erythrocytes were intravenously infected with 2×10^7 *P. falciparum* Pf3D7^{0087/N9}-infected erythrocytes (day 0). Efficacy was assessed by administering one oral dose of N205 (2.5, 5, 15, 30, 50 and 100 mg.kg⁻¹) at day 3 after infection. Treatment group assignments were allocated randomly. Parasitemia was measured by flow cytometry in samples of peripheral blood stained with the fluorescent nucleic acid dye SYTO-16 (Molecular Probes) and anti-murine erythrocyte TER119 monoclonal antibody (Becton Dickinson) in serial 2 μ L blood samples taken every 24 h until assay completion. The ED90 was estimated by fitting a four parameter logistic equation using GraphPad 6.0 Software

3.2. Systemic exposure in infected Pf SCID mice

The levels of N205 were evaluated in whole blood in order to determine standard pharmacokinetic parameters in the individual animals used in the efficacy study. Peripheral blood samples (25 mL) were taken at different times (0.25, 0.5, 1, 2, 4, 6, 8 and 23 h) after drug administration, mixed with 25 μ L of Milli-Q water and immediately frozen on dry ice. The frozen samples were stored at -80 °C until analysis. Vehicle-treated mice experienced the same blood-sampling regimen. Blood samples were processed by liquid-liquid extraction. Quantitative analysis by Liquid chromatography-tandem mass spectrometry (LC-MS/MS) was performed using a Waters UPLC system and Sciex API4000 mass spectrometer. The lower limit of quantification in this assay was 5 ng/mL. Blood concentration vs time was analyzed by non-compartmental analysis (NCA) using Phoenix ver.6.3 (from Pharsight), from which exposure-related values (C_{max} and AUC_{0-23} , AUC_{0-t}) and t_{max} were estimated.

3.3. Chemistry

With exception of those stated all reagents were obtained from commercial suppliers. Dichloromethane, triethylamine and THF were freshly distilled before use. Analytical thin layer chromatography was performed on pre-coated silica gel (0.25 mm layer of silica gel F254) aluminium sheets. UV light (254 nm) was used for all visualizations and flash column chromatography was performed

using Merck 938S Kieselgel 60 Silica gel. IR spectra were run using a Perkin-Elmer 298 infrared spectrophotometer. Solid samples were dissolved in CHCl₃ and liquids/oils applied neat on to sodium chloride discs.

¹H NMR spectra were recorded using a Bruker 400 MHz NMR spectrophotometer. Spectra were referenced to the residual solvent peak and chemical shifts expressed in ppm from TMS as the internal reference peak. All NMR experiments were performed at room temperature. The following annotations are used to describe multiplicity; s, singlet, bs, broad-singlet, d, doublet, t, triplet, q, quartet, m, multiplet and coupling constants are expressed in Hertz.

Mass spectra were recorded between 20 and 70 eV using a VG7070E and/or Micromass LCT mass spectrometers.

3.3.1. Preparation of 4-(4-oxocyclohexyl)phenyl trifluoromethanesulfonate 4b²⁶

To a stirred solution of **4a** (10 g, 52 mmol) in dry DCM (75 mL) at -78 °C was added triethylamine (10 mL). To this mixture was added triflic anhydride (10.6 mL (density = 1.67 g/mL, 63 mmol)) drop-wise over 30 min. After this time the solution was allowed to warm to room temperature and stirred overnight. The reaction mixture was washed with water (30 mL), dried over MgSO₄ and concentrated. Purification by flash column chromatography using ethyl acetate/hexane (20/80) afforded the pure triflate **4b** in 91% yield as off-white foam. ¹H NMR (400 MHz, CDCl₃) δ_H , 1.81–1.99 (m, 2H, CH₂), 2.18–2.28 (m, 2H, CH₂), 2.48–2.58 (m, 4H, CH₂), 3.02–3.15 (m, 1H, CH), 7.22 (d, 2H, $J = 7.2$ Hz, Ar), 7.32 (d, 2H, $J = 7.2$ Hz, Ar). ¹³CNMR (100 MHz, CDCl₃) δ_C 34.2, 41.5, 42.6, 117.6, 121.9, 128.9, 145.7, 148.5, 210.6 MS (ES⁺), [M + Na] (1 0 0), 345.0 HRMS calculated 345.0384 for C₁₃H₁₃O₄Na found 345.0392.

3.3.2. Preparation of methyl 4-(4-oxocyclohexyl)benzoate 4c²⁷

To a solution of the triflate **4b** (2.41 g, 0.007 mol) in DMF (25 mL) and MeOH (12 mL) was added di-isopropylethylamine (2.7 mL) followed by Pd(OAc)₂ (84 mg, 0.376 mmol) and dppp (155 mg, 0.376 mmol). A stream of carbon monoxide (CO) gas was bubbled into the solution for 5 min then a balloon filled with CO was added to the top of the reflux condenser. After allowing to stir for 16 h at 80–90 °C, the reaction mixture was allowed to cool to room temperature, diluted with ethyl acetate (250 mL), washed with saturated bicarbonate solution (50 mL), water (50 mL), brine (50 mL) and dried over sodium sulphate. Purification by flash chromatography (EtOAc/Hex, 20/80) gave **4c** in 72% mp = 94 °C lit²⁷ mp = 93–94 °C ¹H NMR (400 MHz, CDCl₃) δ_H , 1.81–2.04 (m, 2H, CH₂), 2.18–2.28 (m, 2H, CH₂), 2.48–2.58 (m, 4H, CH₂), 3.02–3.15 (m, 1H, CH), 3.90 (s, 3H, CH₃), 7.34 (d, 2H, $J = 7.2$ Hz, Ar), 8.04 (d, 2H, $J = 7.2$ Hz, Ar). ¹³CNMR (100 MHz, CDCl₃) δ_C 34.06, 41.62, 43.2, 52.51, 127.37, 128.97, 130.38, 150.48, 167.24, 211.11, MS (ES⁺), [M + Na] (1 0 0), 255.1 HRMS calculated 255.0997 for C₁₄H₁₆O₃Na found 255.0396.

3.3.3. Alternative Preparation of methyl 4-(4-oxocyclohexyl)benzoate 4c

A solution of oxalyl chloride 4.51 mL (53.3 mmol) in DCM (50 mL) was added to a suspension of 4-phenylcyclohexanone (7g, 40 mmol) and AlCl₃ (16.07 g, 120 mmol) in DCM (150 mL) at 0 °C. The reaction mixture was stirred at 0 °C for 1 h then at room temperature for 2 h. A mixture of methanol (10 mL) and pyridine (8.1 mL) was added drop wise to the reaction mixture and left to stand overnight. The reaction mixture was then washed with water, 3 N HCl, NaHCO₃, dried over NaSO₄, filtered and concentrated. Purification by flash column chromatography gave **4c** in 65% yields with identical spectroscopic and physical properties to that described above.

3.3.4. Preparation of methyl 4-[(1''r,3''r,5''R,7''R)-dispiro[cyclohexane-1,3'-[1,2,4,5]tetraoxane-6',2''-tricyclo[3.3.1.1^{3,7}]decan]-4-yl]benzoate 6a

To a solution of the ketone 4c (4g, 17 mmol) in acetonitrile (75 mL) at 0 °C was added formic acid (8 mL) and 50% H₂O₂ (16 mL). The resulting reaction mixture was allowed to stir for 30 min at 0 °C, then allowed to warm to room temperature and diluted with water (30 mL). The resulting mixture was extracted in DCM (3 x 50 mL), dried over MgSO₄ and concentrated to give the crude gem-bishydroperoxide 5 which was used without further purification. The gem-bishydroperoxide 5 was dissolved in CH₂Cl₂ (50 mL) and added to a stirring solution of the required adamantanone (1.5 equiv.) and rhenium (VII) oxide (0.02 eqv) in CH₂Cl₂ (50 mL) at room temperature. The reaction mixture was stirred for 1 h, filtered through a plug of silica and concentrated. Purification by flash column chromatography gave 6a in 48% as a white foam. ¹H NMR (400 MHz, CDCl₃-d₆) δ_H 7.89 (d, 2H, J = 8.3 Hz, Ar), 7.22 (d, 2H, J = 8.3 Hz, Ar), 3.83 (s, 3H, CH₃), 2.60 (tt, 1H, J = 11.5 Hz, 3.9 Hz, CH), 2.06–1.44 (m, 23H, CH₂/CH) ¹³C NMR (100 MHz, CDCl₃-d₆) δ_C 167.4, 151.6, 130.2, 128.7, 127.3, 111.0, 107.7, 52.5, 44.1, 37.4, 34.7, 33.6, 29.9, 27.5. MS (ES+), [M + Na]⁺ (1 0 0) 437.2

3.3.5. Preparation of 4-[(1''r,3''r,5''R,7''R)-dispiro[cyclohexane-1,3'-[1,2,4,5]tetraoxane-6',2''-tricyclo[3.3.1.1^{3,7}]decan]-4-yl]benzoic acid 6b

A solution of 6a (3.86 mmol) in 10% w/v potassium hydroxide/methanol (12.6 mL) was stirred at reflux for 90 min. The solution was allowed to cool to room temperature and concentrated under reduced pressure. The resulting residue was taken up in water (15 mL) and washed with diethyl ether (3 x 12 mL). The aqueous layer was acidified with concentrated hydrochloric acid and a white precipitate formed. Diethyl ether (18 mL) was added to dissolve the precipitate and the aqueous phase extracted with diethyl ether (2 x 12 mL). The combined organic phases were washed with brine (10 mL), dried over Na₂SO₄, filtered and concentrated under reduced pressure to give a white solid. Recrystallization from ethanol gave the carboxylic acid 6b as a white solid in 91% yield. ¹H NMR (400 MHz, CDCl₃-d₆) δ_H 8.04 (d, 2H, J = 8.4 Hz, Ar), 7.34 (d, 2H, J = 8.4 Hz, Ar), 2.75–2.66 (m, 1H, CH), 2.12–1.45 (m, 22H, CH/CH₂) 171.3, 155.3, 132.8, 131.0, 129.1, 127.3, 126.8, 114.4, 44.5, 36.7, 33.8, 32.9, 27.9, 25.8 MS (ES+), [M - H]⁻ (1 0 0) 399.2 HRMS calculated for 399.1808 C₂₃H₂₇O₆, found 399.1808.

3.3.6. General procedure for the amide formation (7a-j)

To a solution of the acid **6b** (2.33 mmol) in dry DCM (30 mL) was added triethylamine (0.7 mmol, 1.5 eq) and ethylchloroformate (2.33 mmol, 1.0 eq). The reaction was allowed to stir for 60 min at 0 °C. (2.33 mmol, 1.0 eq) of the required amine was added, and after stirring for 30 min, the reaction mixture was allowed to warm to room temperature and then allowed to stir for a further 90 min. The reaction mixture was then diluted with water and extracted with DCM (3 x 30 mL). The combined organic extracts were washed with brine, dried over anhydrous Na₂SO₄ and concentrated. Purification by flash column chromatography afforded the required amide.

3.3.7. Preparation of 4-[(1''r,3''r,5''R,7''R)-dispiro[cyclohexane-1,3'-[1,2,4,5]tetraoxane-6',2''-tricyclo[3.3.1.1^{3,7}]decan]-4-yl]phenyl(morpholin-4-yl)methanone 7a

White solid (Yield 87%) Mpt = 123–124 °C ¹H NMR (400 MHz, CDCl₃) δ_H 7.38 (d, 2H, J = 8 Hz, Ar), 7.29 (d, 2H, J = 8 Hz, Ar), 3.4–3.9 (m, 4H, CH₂), 3.14–3.40 (m, 2H, CH), 2.6–2.7 (m, 1H, CH), 1.60–2.10 (m, 20H, CH₂/CH), ¹³C NMR (100 MHz, CDCl₃) δ_C 170.9, 169.5, 148.3, 127.8, 127.4, 117.7, 110.9, 107.8, 67.3, 43.9, 39.6, 37.6, 34.7, 33.6, 32.3, 30.6, 29.9, 27.8 MS (ES+), [M + Na]⁺ 492.2 (1 0 0), HRMS calculated for 292.2362 C₂₇H₃₅NO₆Na found,

492.2372% C, H, N calculated; C = 69.06, H = 7.51, N = 2.98; found C = 69.40, H = 7.85, N = 3.21

3.3.8. Preparation of 4-[(1''r,3''r,5''R,7''R)-dispiro[cyclohexane-1,3'-[1,2,4,5]tetraoxane-6',2''-tricyclo[3.3.1.1^{3,7}]decan]-4-yl]-N-(piperidin-4-ylmethyl)benzamide 7b

Off white powder (Yield 77%) Mpt = 132–134 °C ¹H NMR (400 MHz, CDCl₃-d₆) δ_H 8.41 (t, 1H, J = 5.9 Hz, NH), 7.77 (d, 2H, J = 8.3 Hz, Ar), 7.32 (d, 2H, J = 8.3 Hz, Ar), 3.11 (t, 2H, J = 5.9 Hz, NCH₂), 2.98 (t, 4H, J = 10.6 Hz, CH₂N), 2.83 (t, 2H, J = 6.3 Hz, CH₂), 2.78–2.70 (m, 1H, CH), 2.55–2.45 (m, 1H, CH), 1.95–0.94 (m, 26H, CH/CH₂) ¹³C NMR (100 MHz, CDCl₃-d₆) δ_C 177.5, 149.2, 133.0, 127.7, 126.9, 110.1, 107.6, 51.5, 46.5, 45.3, 42.5, 40.5, 38.8, 36.6, 32.9, 29.9, 27.2, 26.8 MS (ES+), [M + H]⁺ (1 0 0) 497.3 HRMS calculated for 497.3015 C₂₉H₄₁N₂O₅, found 497.3017; % C, H, N calculated; C = 70.13, H = 8.12, N = 5.64; found C = 70.05, H = 7.95, N = 5.42

3.3.9. Preparation of 4-[(1''r,3''r,5''R,7''R)-dispiro[cyclohexane-1,3'-[1,2,4,5]tetraoxane-6',2''-tricyclo[3.3.1.1^{3,7}]decan]-4-yl]-N-[2-(methylamino)ethyl]benzamide 7c

White foam (Yield, 64%) Mpt 60–62 °C ¹H NMR (400 MHz, CDCl₃-d₆) δ_H 8.81 (t, 1H, J = 5.5 Hz, NH), 7.88 (d, 2H, J = 8.2 Hz, Ar), 7.40 bs, 1H, NH), 7.34 (d, 2H, J = 8.2 Hz, Ar), 3.60 (q, 2H, J = 5.9 Hz, NCH₂), 3.07 (t, 2H, J = 5.9 Hz, CH₂N), 2.79–2.72 (m, 1H, CH), 2.56 (s, 3H, NCH₃), 1.99–1.57 (m, 22H, CH/CH₂) MS (ES+), [M + H]⁺ (1 0 0) 457.3 HRMS calculated for 457.2702 C₂₆H₃₇N₂O₅, found 457.2701% C, H, N Calculated; C = 68.40, H = 7.95, N = 6.14; found C = 68.10, H = 7.62, N = 5.92

3.3.10. Preparation of N-(3-aminocyclobutyl)-4-[(1''r,3''r,5''R,7''R)-dispiro[cyclohexane-1,3'-[1,2,4,5]tetraoxane-6',2''-tricyclo[3.3.1.1^{3,7}]decan]-4-yl]benzamide 7d

White foam (Yield 82%) Mpt = 116–118 °C ¹H NMR (400 MHz, CDCl₃-d₆) δ_H 8.74 (s, 1H, NH), 7.88 (bs, 2H, NH₂), 7.56 (d, 2H, J = 8.3 Hz, Ar), 7.34 (d, 2H, J = 8.3 Hz, Ar), 3.55–3.50 (m, 1H, CH), 3.45–3.24 (m, 5H, CH/CH₂), 3.20–3.18 (m, 1H, CH), 1.99–1.52 (m, CH/CH₂) ¹³C NMR (100 MHz, CDCl₃-d₆) δ_C 169.5, 149.4, 128.2, 127.0, 110.1, 107.5, 42.5, 40.7, 36.5, 32.9, 31.5, 26.8 MS (ES+), [M + H]⁺ (1 0 0) 455.3 HRMS calculated for 455.2546 C₂₆H₃₅N₂O₅, found 455.2532% C, H, N Calculated; C = 69.21, H = 7.74, N = 5.98; found C = 69.01, H = 7.38, N = 5.63

3.3.11. Preparation of 4-[(1''r,3''r,5''R,7''R)-dispiro[cyclohexane-1,3'-[1,2,4,5]tetraoxane-6',2''-tricyclo[3.3.1.1^{3,7}]decan]-4-yl]phenyl(thiomorpholin-4-yl)methanone 7e

White solid (Yield 76%) ¹H NMR (400 MHz, CDCl₃) δ_H 7.40 (d, 2H, J = 8 Hz, Ar), 7.27 (d, 2H, J = 8 Hz, Ar), 3.4–3.9 (m, 4H, CH₂), 3.14–3.40 (m, 2H, CH), 2.58–2.7 (m, 1H, CH), 1.60–2.10 (m, 20H, CH₂/CH), ¹³C NMR (100 MHz, CDCl₃) δ_C 170.8, 169.5, 148.3, 133.6, 127.8, 127.4, 110.9, 107.7, 43.9, 42.9, 39.6, 37.3, 34.6, 33.6, 32.2, 30.5, 27.8, 27.5 MS (ES+), [M + Na]⁺ 508.2 (1 0 0), HRMS calculated for 508.2134 C₂₇H₃₅NO₅NaS found, 508.2138% C, H, N Calculated; C = 66.78, H = 7.26, N = 2.88; found C = 66.39, H = 6.98, N = 2.47

3.3.12. Preparation of 4-[(1''r,3''r,5''R,7''R)-dispiro[cyclohexane-1,3'-[1,2,4,5]tetraoxane-6',2''-tricyclo[3.3.1.1^{3,7}]decan]-4-yl]phenyl(4-methylpiperazin-1-yl)methanone 7f

White solid (Yield 81%) mpt 108–110 °C ¹H NMR (400 MHz, CDCl₃) δ_H 7.4 (d, 2H, J = 9 Hz, Ar), 7.27 (d, 2H, J = 9 Hz, Ar), 3.4–3.9 (m, 4H, CH₂), 3.14–3.34 (m, 2H, CH), 2.6–2.8 (m, 1H, CH), 2.42 (s, 3H, CH₃), 1.50–2.10 (m, 20H, CH₂/CH) ¹³C NMR (100 MHz, CDCl₃) δ_C 170.4, 150.6, 147.9, 133.2, 129.9, 127.3, 127.0, 126.7, 110.5, 107.3, 45.0, 43.6, 43.4, 41.2, 34.2, 33.1, 31.7, 29.5, 27.0 MS (ES+), [M + H]⁺ 483.3 (1 0 0), HRMS calculated for 483.2859 C₂₈H₃₉N₂O₅ found, 483.2858% C, H, N Calculated; C = 69.68, H = 7.94, N = 5.80; found C = 69.41, H = 7.42, N = 5.49

3.3.13. Preparation of 1,4-diazepan-1-yl{4-[(1''r,3''r,5''R,7''R)-dispiro[cyclohexane-1,3'-[1,2,4,5]tetroxane-6',2''-tricyclo[3.3.1.1^{3,7}]decan]-4-yl]phenyl}methanone 7g

White powder (Yield 58%) ¹H NMR (400 MHz, CDCl₃) δ_H, 7.24–7.4 (m, 4H, Ar), 3.5–3.8 (m, 6H, CH/CH₂), 3.1–3.4 (m, 4H, CH), 2.65–2.57 (m, 1H, CH), 1.48–2.11 (m, 22H, CH₂/CH), ¹³C NMR (100 MHz, CDCl₃) δ_C 172.2, 147.8, 134.9, 127.4, 127.1, 126.8, 110.9, 107.8, 80.2, 45.2, 43.8, 29.9, 28.8, 27.5, 27.0 MS (ES⁺), [M + H] 483.3 (1 0 0), HRMS calculated for 483.2859 C₂₈H₃₉N₂O₅ found, 483.2856% C, H, N calculated; C = 69.68, H = 7.94, N = 5.80; found C = 69.41, H = 7.65, N = 5.51

3.3.14. Preparation of {4-[(1''r,3''r,5''R,7''R)-dispiro[cyclohexane-1,3'-[1,2,4,5]tetroxane-6',2''-tricyclo[3.3.1.1^{3,7}]decan]-4-yl]phenyl} (piperazin-1-yl)methanone 7h

White solid (Yield 78%) ¹H NMR (400 MHz, CDCl₃) δ_H, 7.24–7.41 (m, 4H, Ar), 3.8–4.2 (m, 4H, CH₂), 3.1–3.4 (m, 2H, CH), 2.6–2.8 (m, 1H, CH), 1.50–2.2 (m, 20H, CH₂/CH), ¹³C NMR (100 MHz, CDCl₃) δ_C, 171.4, 156.1, 148.9, 132.9, 128.0, 127.7, 110.9, 107.7, 66.2, 53.3, 43.9, 42.5, 37.3, 33.6, 30.2, 27.4 MS (ES⁺), [M + H] 469.3 (1 0 0), HRMS calculated for 468.2624 C₂₇H₃₇N₂O₅ found, 468.2631% C, H, N calculated; C = 69.21, H = 7.74, N = 5.98; found C = 69.36, H = 7.85, N = 5.61

3.3.15. Preparation of (4-aminopiperidin-1-yl){4-[(1''r,3''r,5''R,7''R)-dispiro[cyclohexane-1,3'-[1,2,4,5]tetroxane-6',2''-tricyclo[3.3.1.1^{3,7}]decan]-4-yl]phenyl}methanone 7i

White powder (Yield 86%) Mpt = 116–118 °C. ¹H NMR (400 MHz, CDCl₃) δ_H, 7.24–7.4 (m, 4H, Ar), 3.7–4.1 (m, 7H, CH/CH₂), 3.1–3.4 (m, 4H, CH), 2.6 (m, 1H, CH), 1.60–2.1 (m, 20H, CH₂/CH), ¹³C NMR (100 MHz, CDCl₃) δ_C 172.0, 155.6, 149.3, 132.2, 128.0, 127.9, 126.7, 110.9, 107.7, 53.7, 43.9, 43.8, 41.1, 37.3, 33.5, 27.4 MS (ES⁺), [M + H] 483.3 (1 0 0), HRMS calculated for 483.2814 C₂₈H₃₉N₂O₅ found, 483.2805% C, H, N Calculated; C = 69.68, H = 7.94, N = 5.80; found C = 69.41, H = 7.81, N = 5.71

3.3.16. Preparation of N-(2-aminoethyl)-4-[(1''r,3''r,5''R,7''R)-dispiro[cyclohexane-1,3'-[1,2,4,5]tetroxane-6',2''-tricyclo[3.3.1.1^{3,7}]decan]-4-yl]benzamide 7j

White powder (Yield, 76%). ¹H NMR (400 MHz, CDCl₃-d₆) δ_H 8.74 (t, 1H, J = 5.5 Hz, NH), 8.12 (bs, 2H, NH₂), 7.86 (d, 2H, J = 8.3 Hz, Ar), 7.34 (d, 2H, J = 8.3 Hz, Ar), 3.52 (q, 2H, J = 5.8 Hz, NCH₂), 2.97 (t, 2H, J = 5.8 Hz, CH₂N), 2.80–2.71 (m, 1H, CH), 1.99–1.52 (m, 22H, CH/CH₂) ¹³C NMR (100 MHz, CDCl₃-d₆) δ_C 167.3, 157.1, 149.8, 132.0, 128.4, 110.3, 107.8, 52.4, 42.5, 41.1, 38.9, 37.5, 35.6, 33.5, 32.8, 28.9, 27.1, 26.8 MS (ES⁺), [M + H]⁺ (1 0 0) 443.3 HRMS calculated for 443.2546 C₂₅H₃₅N₂O₅, found 443.2545% C, H, N calculated; C = 67.85, H = 7.74, N = 6.33; found C = 67.40, H = 7.34, N = 6.21

3.3.17. Preparation of {4-[(1''r,3''r,5''R,7''R)-dispiro[cyclohexane-1,3'-[1,2,4,5]tetroxane-6',2''-tricyclo[3.3.1.1^{3,7}]decan]-4-yl]phenyl} methanol 8

To a stirred solution at 0 °C of methyl benzoate 6 (1.5 g, 3.65 mmol) in THF (50 mL) was added LiAlH₄ (0.28 g, 7.29 mmol). The suspension was allowed to stir at 0 °C and was monitored by TLC to determine the consumption of the benzoate. The reaction mixture was quenched with 1 N HCl and was then extracted with ethyl acetate (3 x 50 mL). The combined organic layers were dried over anhydrous sodium sulphate, filtered and concentrated under reduced pressure. Purification by flash column chromatography afforded the required alcohol 8 as a white powder (1.36 g, 97%). ¹H NMR (400 MHz, CDCl₃-d₆) δ_H 7.27 (d, 2H, J = 8.2 Hz, Ar), 7.21 (d, 2H, J = 8.2 Hz, Ar), 4.62 (s, 2H, ArCH₂OH), 2.62 (tt, 1H, J = 11.4 Hz, 4.0 Hz, Ar), 2.08–1.57 (m, 22H, CH₂/CH) ¹³C NMR (100 MHz, CDCl₃-d₆) δ_C 145.9, 139.3, 127.6, 110.9, 107.9, 65.6, 60.8, 43.8,

37.4, 36.2, 34.7, 33.6, 30.1, 27.5 MS (ES⁺), [M + Na]⁺ (1 0 0) 409.2 HRMS 409.1991 calculated for C₂₃H₃₀NO₅Na found 409.1990.

3.3.18. Preparation of 4-[(1''r,3''r,5''R,7''R)-dispiro[cyclohexane-1,3'-[1,2,4,5]tetroxane-6',2''-tricyclo[3.3.1.1^{3,7}]decan]-4-yl]benzyl methanesulfonate 9

Methanesulfonyl chloride (3.36 mmol) and triethylamine (3.62 mmol) were added at 0 °C under nitrogen atmosphere to a solution of 8 (1.81 mmol) in dry DCM (50 mL). The mixture was allowed to stir for 60 min at the same temperature, washed with aqueous 5% NaHCO₃ and water, and dried over Na₂SO₄. Evaporation of the solvent gave the mesylate 9 as colourless oil (0.8, 95%). ¹H NMR (400 MHz, CDCl₃-d₆) δ_H 7.36 (d, 2H, 8.1 Hz, Ar), 7.27 (d, 2H, J = 8.1 Hz, Ar), 5.21 (s, 2H, CH₂O), 2.92 (s, 3H, SO₂CH₃), 2.64 (tt, 1H, J = 11.4 Hz, 3.8 Hz, CH), 2.09–1.56 (m, 22H, CH₂/CH) MS (ES⁺), [M + Na]⁺ (1 0 0) 487.3 HRMS calculated for 487.1766 C₂₄H₃₂NO₇Na, found 487.1765.

3.3.19. General procedure for the amine formation (10a-b)

To a solution of mesylate 9 (1.08 mmol 1 eq) in dichloromethane (25 mL) were added triethylamine (2.15 mmol, 2 eq) followed by the amine (2.15 mmol 2, eq) at 0 °C temperature. The reaction mixture was stirred at room temperature over a period of 12 h. The resulting reaction mixture was diluted with dichloromethane (50 mL), washed with water (3 x 20 mL), brine (10 mL) and dried over sodium sulphate. The crude product obtained was purified by flash column chromatography to the required amine.

3.3.20. Preparation of 4-[(1''r,3''r,5''R,7''R)-dispiro[cyclohexane-1,3'-[1,2,4,5]tetroxane-6',2''-tricyclo[3.3.1.1^{3,7}]decan]-4-yl]benzyl)morpholine 10a (N205)

White powder (Yield, 62%). Mtp 138–140 °C. ¹H NMR (400 MHz, CDCl₃-d₆) δ_H 7.24 (d, 2H, J = 8.1 Hz, Ar), 7.17 (d, 2H, J = 8.1 Hz, Ar), 3.73–3.68 (m, 4H, NCH₂), 3.46 (s, 2H, ArCH₂N), 2.67–2.54 (m, 1H, CH), 2.43 (bs, 4H, CH₂O), 2.09–1.58 (m, 22H, CH/CH₂) ¹³C NMR (100 MHz, CDCl₃-d₆) δ_C 145.2, 136.0, 129.7, 127.1, 110.9, 107.9, 67.4, 63.6, 54.0, 43.8, 37.4, 34.8, 33.6, 33.4, 32.3, 30.1, 27.5 MS (ES⁺), [M + H]⁺ (1 0 0) 456.3 HRMS calculated for 456.2750 C₂₇H₃₈NO₅, found 456.2762; C₂₈H₃₉NO₄F, found 472.2859% C, H, N Calculated; C = 71.18, H = 8.18, N = 3.07; found C = 70.92, H = 7.99, N = 3.10

3.3.21. Preparation of 1-{4-[(1''r,3''r,5''R,7''R)-dispiro[cyclohexane-1,3'-[1,2,4,5]tetroxane-6',2''-tricyclo[3.3.1.1^{3,7}]decan]-4-yl]benzyl}-4-fluoropiperidine 10b

White powder (Yield, 60%), Mtp 122–124 °C ¹H NMR (400 MHz, CDCl₃-d₆) δ_H 7.23 (d, 2H, J = 8.1 Hz, Ar), 7.17 (d, 2H, J = 8.1 Hz, Ar), 4.79–4.53 (m, 1H, CHF), 3.46 (s, 2H, CH₂N), 2.64–2.53 (m, 5H, NCH₂/CH), 2.40–2.31 (m, 4H, CH₂), 2.06–1.54 (m, 22H, CH₂/CH) ¹³C NMR (100 MHz, CDCl₃-d₆) δ_C 145.1, 136.6, 129.6, 127.1, 110.9, 107.9, 90.0, 88.3, 63.1, 50.0, 43.8, 37.4, 34.7, 33.6, 32.3, 31.9, 30.6, 27.5 MS (ES⁺), [M + H]⁺ (1 0 0) 472.3 HRMS calculated for 472.2863 C₂₈H₃₉NO₄F, found 472.2859% C, H, N Calculated; C = 71.31, H = 8.12, N = 4.03; found C = 70.97, H = 7.91, N = 3.80

3.3.22. Preparation of 4-[(1''r,3''r,5''R,7''R)-dispiro[cyclohexane-1,3'-[1,2,4,5]tetroxane-6',2''-tricyclo[3.3.1.1^{3,7}]decan]-4-yl]benzyl)morpholine Mesylate

0.3 mmol of 10a was dissolved in 2 mL of anhydrous diethyl ether and 1.5 mmol of 100 mM methane sulfonic acid stock solution was added. The precipitate formed was collected, washed with diethyl ether and air dried to give the titled salt. White powder (Yield 70%). Mtp 158–160 °C ¹H NMR (400 MHz, DMSO d₆) δ_H 9.76 (s, 1H, NH), 7.44 (d, 2H, J = 8.2 Hz, Ar), 7.37 (d, 2H, J = 8.1 Hz, Ar), 4.31 (d, 2H, J = 5.0 Hz, CH₂), 3.96 (d, 2H, J = 10.3 Hz, CH₂), 3.62 (t, 2H, J = 11.6 Hz, CH₂), 3.26 (d, 2H, J = 11.9 Hz, CH₂), 3.18–

3.03 (m, 4H, CH₂), 2.78–2.69 (m, 1H, CH), 2.35 (s, 3H, SO₂CH₃), 1.96–1.51 (m, 22H, CH/CH₂) MS (ES+), [M + H]⁺ (1 0 0) 456.3 HRMS calculated for 456.2750 C₂₇H₃₈NO₅, found 456.2762.% C, H, N calculated; C = 60.96, H = 7.49, N = 2.54; found C = 60.88, H = 7.40, N = 2.21

3.3.23. Preparation of 1-{4-[(1''r,3''r,5''R,7''R)-dispiro[cyclohexane-1,3'-[1,2,4,5]tetraoxane-6',2''-tricyclo[3.3.1.1^{3,7}]decan]-4-yl]benzyl]-4-fluoropiperidine mesylate

0.3 mmol 10b was dissolved in 2 mL of anhydrous diethyl ether and 1.5 mmol of methane sulfonic acid stock solution was added. The precipitate formed was collected, washed with diethyl ether and air dried to give the titled salt. White powder (Yield 68%). Mpt 108–110 °C ¹H NMR (400 MHz, DMSO d₆) δ_H 9.41 (s, 1H, NH), 7.44 (d, 2H, J = 8.1 Hz, Ar), 7.36 (d, 2H, J = 8.1 Hz, Ar), 5.07–4.70 (m, 1H, CHF), 4.32 (d, 2H, J = 5.1 Hz, CH₂), 3.27 (d, 2H, J = 11.1 Hz, CH₂), 3.19–2.96 (m, 4H, CH₂), 2.79–2.66 (m, 1H, CH), 2.38 (a, 3H, SO₂CH₃), 2.15–1.96 (m, 2H, CH₂), 1.95–1.50 (m, 22H, CH/CH₂) MS (ES+), [M + H]⁺ (1 0 0) 472.3 HRMS calculated for 472.2863 C₂₈H₃₉NO₄F, found 472.2859.% C, H, N Calculated; C = 71.31, H = 8.12, N = 2.97; found C = 71.02, H = 8.01, N = 2.68

4. Conclusion

N205 represents a molecule with a vastly improved overall profile compared to the first generation tetraoxane RKA182 with comparable antimalarial potency compared to OZ439. Whilst data with human liver microsomes and human blood indicate similar levels of stability compared to OZ439, the latter has superior in rodent *in vitro* microsomal and blood stability and *in vivo* rat PK profiles. Data obtained in the *Pf* SCID mouse model for N205 were extremely encouraging and suggest that the benzylamino tetraoxane template **2** should be explored further to enhance the solubility, metabolic and blood stability even further. A recent paper by Venerstom et al. has examined a series of analogues of OZ439 to determine the key features that impart *in vivo* potency in the mouse model of malaria; the conclusion from this work is that whilst prolonged plasma exposure is important for curative activity, there are other factors involved in imparting high efficacy in rodent models.⁸ This observation provides an additional key challenge in understanding the dynamics of this class of drug.

Acknowledgements

Funding: This work was supported by grants from the European Union (Antimal, SAW, PON, EU FP6), the Medicines for Malaria Venture (SAW, PMO, GB). The authors would also like to thank Dr Sergio Wittlin and Christoph Fischli (Swiss Tropical and Public Health Institute Socinstrasse 57, 4051 Basel, Switzerland) for the data recorded in Table 2 (*P. berghei* mouse model).

A. Supplementary data

Supplementary data associated with this article can be found, in the online version, at <https://doi.org/10.1016/j.bmc.2018.05.006>.

References

1. WHO, Global report on antimalarial drug efficacy and drug resistance: 2000–2010, 2010.

2. Dondorp AM, Nosten F, Yi P, et al. Artemisinin resistance in *Plasmodium falciparum* malaria. *New Engl J Med*. 2009;361:455–467.
3. Leang R, Taylor WR, Bouth DM, et al. Evidence of *Plasmodium falciparum* Malaria Multidrug Resistance to Artemisinin and Piperaquine in Western Cambodia: Dihydroartemisinin-Piperaquine Open-Label Multicenter Clinical Assessment. *Antimicrob Agents Chemotherapy*. 2015;59:4719–4726.
4. Noedl H, Se Y, Schaefer K, et al. Resistance in Cambodia 1 Study, Evidence of artemisinin-resistant malaria in western Cambodia. *New Engl J Med*. 2008;359:2619–2620.
5. Dong Y, Wittlin S, Sriraghavan K, et al. The Structure-Activity Relationship of the Antimalarial Ozonide Arterolane (OZ277). *J Med Chem*. 2010;53:481–491.
6. Valecha Neena, Krudsood Srivicha, Tangpukdee Noppadon, Mohanty Sanjib, Sharma SK, Tyagi PK, Anvikar Anupkumar, Mohanty Rajesh, Rao BS, Jha AC, Shahi B, Narayan Singh Jai Prakash, Roy Arjun, Kaur Pawandeep, Kothari Shantanu, Mehta Shantanu, Gautam Anirudh, Paliwal Jyoti K, Arora Sudershan, Saha Nilanjan. Arterolane maleate plus piperaquine phosphate for treatment of uncomplicated *Plasmodium falciparum* malaria: A comparative, multicenter, randomized clinical trial. *Clin Infect Dis*. 2012;55(5):663–671. <https://doi.org/10.1093/cid/cis475>.
7. Charman SA, Arbe-Barnes S, Bathurst IC, et al. Synthetic ozonide drug candidate OZ439 offers new hope for a single-dose cure of uncomplicated malaria. *Proc Natl Acad Sci USA*. 2011;108:4400–4405.
8. Dong Y, Wang X, Kamaraj S, et al. Structure-Activity Relationship of the Antimalarial Ozonide Artefenomel (OZ439). *J Med Chem*. 2017;60:2654–2668.
9. Kim HS, Hammill JT, Guy RK. Seeking the Elusive Long-Acting Ozonide: Discovery of Artefenomel (OZ439). *J Med Chem*. 2017;60:2651–2653.
10. Ellis GL, Amewu R, Sabbani S, et al. Two-Step Synthesis of Achiral Spiro-1,2,4,5-tetraoxanes with Outstanding Antimalarial Activity, Low Toxicity, and High-Stability Profiles. *J Med Chem*. 2008;51:2170–2177.
11. Fisher LC, Blackie MAL. Tetraoxanes as Antimalarials: Harnessing the Endoperoxide. *Mini-Rev Med Chem*. 2014;14:123–135.
12. Kumar N, Khan SI, Atheaya H, Mangain R, Rawat DS. Synthesis and *in vitro* antimalarial activity of tetraoxane-amine/amide conjugates. *Eur J Med Chem*. 2011;46:2816–2827.
13. Kumar N, Khan SI, Rawat DS. Synthesis and Antimalarial-Activity Evaluation of Tetraoxane-Triazine Hybrids and Spiro[piperidine-4,3'-tetraoxanes]. *Helv Chim Acta*. 2012;95:1181–1197.
14. Kumar N, Singh R, Rawat DS. Tetraoxanes: Synthetic and Medicinal Chemistry Perspective. *Med Res Rev*. 2012;32:581–610.
15. Opsenica D, Pocsfalvi G, Milhous WK, Solaja BA. Antimalarial peroxides: the first intramolecular 1,2,4,5-tetraoxane. *J Serb Chem Soc*. 2002;67:465–471.
16. O'Neill PM, Amewu RK, Nixon GL, et al. Identification of a 1,2,4,5-tetraoxane antimalarial drug-development candidate (RKA 182) with superior properties to the semisynthetic artemisinins. *Angew Chem Int Ed Engl*. 2010;49:5693–5697.
17. O'Neill PM, Sabbani S, Nixon GL, et al. Optimisation of the synthesis of second generation 1,2,4,5 tetraoxane antimalarials. *Tetrahedron*. 2016;72:6118–6126.
18. O'Neill PM, Amewu RK, Sabbani S, et al. A tetraoxane-based antimalarial drug candidate that overcomes PfK13-C580Y dependent artemisinin resistance. *Nat Commun*. 2017;8:15159.
19. Ghorai P, Dussault PH. A new peroxide fragmentation: efficient chemical generation of (1O2) in organic media. *Org Lett*. 2009;11:4572–4575.
20. Smilkstein M, Sriwilaijaroen N, Kelly JX, Wilairat P, Riscoe M. Simple and inexpensive fluorescence-based technique for high-throughput antimalarial drug screening. *Antimicrob Agents Chemotherapy*. 2004;48:1803–1806.
21. Wang XF, Dong YX, Wittlin S, et al. Comparative Antimalarial Activities and ADME Profiles of Ozonides (1,2,4-trioxolanes) OZ277, OZ439, and Their 1,2-Dioxolane, 1,2,4-Trioxane, and 1,2,4,5-Tetraoxane Isosteres. *J Med Chem*. 2013;56:2547–2555.
22. Neely MN, van Guilder MG, Yamada WM, Schumitzky A, Jelliffe RW. Accurate detection of outliers and subpopulations with Pmetrics, a nonparametric and parametric pharmacometric modeling and simulation package for R. *Ther Drug Monit*. 2012;34:467–476.
23. Angulo-Barturen I, Jimenez-Diaz MB, Mulet T, et al. A murine model of falciparum-malaria by *in vivo* selection of competent strains in non-myelodepleted mice engrafted with human erythrocytes. *PLoS one*. 2008;3:e2252.
24. Jimenez-Diaz MB, Mulet T, Viera S, et al. Improved Murine Model of Malaria Using *Plasmodium falciparum* Competent Strains and Non-Myelodepleted NOD-scid IL2R gamma(null) Mice Engrafted with Human Erythrocytes. *Antimicrob Agents Chemotherapy*. 2009;53:4533–4536.
25. Younis Y, Douelle F, Feng TS, et al. 3,5-Diaryl-2-aminopyridines as a Novel Class of Orally Active Antimalarials Demonstrating Single Dose Cure in Mice and Clinical Candidate Potential. *J Med Chem*. 2012;55:3479–3487.
26. Tan JQ, Kim RM, Mirc JW. Preparation of biphenylpyridine compounds as soluble guanylate cyclase activators. USA: Merck Sharp & Dohme Corp; 2012. 115.
27. DeGraw JI, Christie PH, Colwell WT, Sirotnak FM. Synthesis and antifolate properties of 5,10-ethano-5,10-dideazaaminopterin. *J Med Chem*. 1992;35:320–324.